10th IAA SYMPOSIUM
ON SMALL SATELLITES
FOR EARTH OBSERVATION

Proceedings

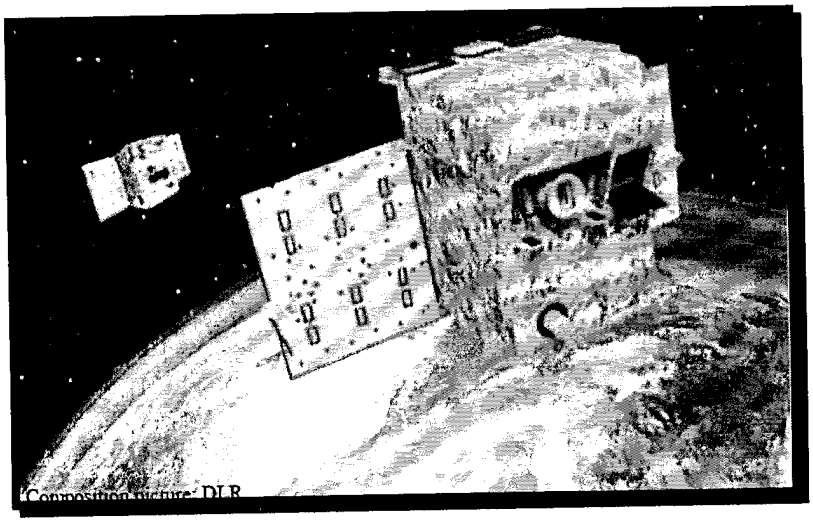

April 20 – 24, 2015

BBAW,
Gendarmenmarkt

BERLIN, GERMANY

International Academy of Astronautics

Supported and hosted by

DLR Deutsches Zentrum für Luft- und Raumfahrt e.V.

Institute of Optical Sensor Systems

START

Attitude estimation, control and momentum dumping: a case study for CONASAT

H. K. Kuga[1], P. M. Bringhenti[1], V. Carrara[1]

[1] Instituto Nacional de Pesquisas Espaciais, Av dos Astronautas 1758, 12227-010 São José dos Campos/SP, Brasil

Abstract: This paper presents the attitude estimation using Kalman filter, the PID control strategy and the momentum dumping technique using magnetorquers for the Brazilian satellite CONASAT. Attitude will be represented in quaternions, so the Kalman filter will be implemented using the reduced order covariance, to avoid the singularity of the covariance matrix. The reaction wheel desaturation will be made using the Conventional Cross Product Law (CCPL) and a bang-bang strategy, for comparison by means of the magnetorquers. The results show that the Kalman filter estimates correctly the gyroscope bias, allowing the PID controller to keep the attitude error below 5°, even during the satellite passage through the Earth's shadow. The wheel's speed decreased to the reference value (zero) in about 4500s, using either CCPL or the bang-bang strategy.

1 INTRODUCTION

Earth-pointed satellites must maintain a fixed attitude even in the presence of disturbances. In many applications, a high precision pointing is achieved using reaction wheels as actuators, which are used as momentum storage for the spacecraft, but are limited to the compensation of internal and periodical external torques only [1].

Secular torques, such as aerodynamic drag and solar radiation pressure, tend to saturate the reaction wheels, and an external torque is necessary to drive the wheel's speed back to operational levels. Therefore, an adequate control law is required to minimize the influence of disturbance torques, allowing the nominal operation of the wheels.

The Brazilian CONASAT [2] satellite is under design at the National Institute of Space Research (INPE), and consists of 8U CubeSat configuration, illustrated in Figure 1. All subsystems are housed in a 2U configuration, with another 2U used for cold redundancy. The remaining 4U are empty but they provide extra power generation with their solar panels [3]. Each CONASAT uses directional antennas for payload that requires nadir pointing within 5° accuracy. The satellite shall be equipped with MEMS gyroscopes, magnetic sensors, sun sensors, reaction wheels and magnetorquers.

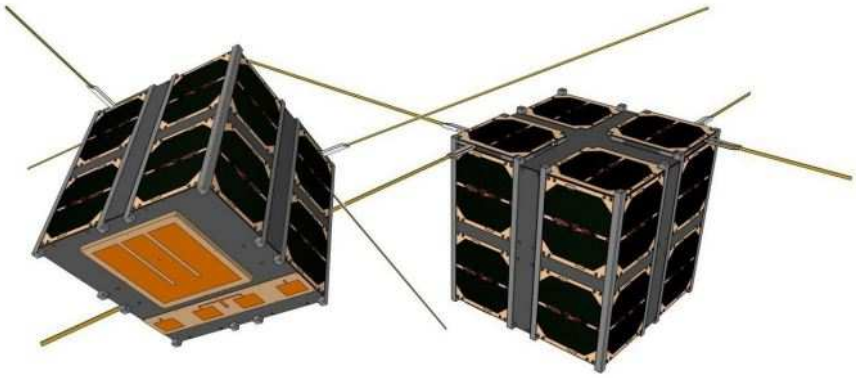

Figure 1: CONASAT configuration

2 EQUATIONS OF MOTION AND ATTITUDE CONTROL STRATEGY

In this work, the attitude is represented by quaternion, because it does not have limitations due to singularities and trigonometric functions, requiring less computational effort. The downside is that it does not have a direct physical interpretation, so usually the calculations are done using quaternions and then transformed to Euler angles. The quaternion can be calculated as [4][5]:

$$\mathbf{q} = \begin{pmatrix} \boldsymbol{\varepsilon} & \eta \end{pmatrix}, \tag{1}$$

where $\boldsymbol{\varepsilon}$ is the vector part, η the scalar, and are defined as functions of Euler angle (θ) and axis ($\mathbf{a}$):

$$\boldsymbol{\varepsilon} = \mathbf{a}\,\mathrm{sen}\,\frac{\theta}{2},\ \eta = \frac{\cos\theta}{2} \tag{2}$$

The kinematic differential equation of the satellite can be described as:

$$\dot{\mathbf{q}} = \frac{1}{2}\boldsymbol{\Omega}\,\mathbf{q}, \tag{3}$$

where [6]

$$\boldsymbol{\Omega} = \begin{pmatrix} -\boldsymbol{\omega}^{\times} & \boldsymbol{\omega} \\ -\boldsymbol{\omega}^{T} & 0 \end{pmatrix}, \tag{4}$$

is the matrix representation of the 4th order vector product of the angular velocities, and $\boldsymbol{\omega}^{\times}$ is the 3th order matrix of the angular velocity vector $\boldsymbol{\omega}$ cross product, such that $\boldsymbol{\omega}^{\times}\,\mathbf{v} = \boldsymbol{\omega} \times \mathbf{v}$

The satellite dynamic equation, considering a set of three reaction wheels and magnetorquers aligned with the satellite's principal inertia axis, is given by:

$$\mathbf{I}\dot{\boldsymbol{\omega}} = (\mathbf{I}\boldsymbol{\omega} + \mathbf{h}_r) \times \boldsymbol{\omega} + \mathbf{T}_{ext} - \mathbf{T}_r, \tag{5}$$

where $\mathbf{I}$ is the satellite inertia matrix, $\boldsymbol{\omega}$ is the angular velocity, $\mathbf{h}_r$ is the reaction wheel's angular momentum, $\mathbf{T}_r$ is the net reaction wheel torque and $\mathbf{T}_{ext}$ is the external torques, including disturbance torques and magnetorquer control torque.

Attitude determination will be performed using a TRIAD algorithm based on measurements of a 3-axis magnetometer and coarse sun sensors. The TRIAD algorithm computes the attitude of a reference system constructed by the cross product of two non aligned vectors, assuming that one of the axis is aligned with one of the input vectors. The satellite attitude is then computed by applying the TRIAD on two vector pairs: the sensor readings and a onboard computed mathematical model of the Earth's magnetic field and the Sun direction in an inertial reference frame.

The adopted attitude control strategy, considering a set of three reaction wheels, was a PID controller [3], computed by:

$$\mathbf{u}_k = -k_p\,\boldsymbol{\theta}_k - k_i \sum_{i=0}^{k} \boldsymbol{\theta}_i\,\Delta t - k_d\,\boldsymbol{\omega}_k\,, \tag{6}$$

where k_p, k_i e k_d are, respectively, the proportional, integral and derivative gains, adjusted to 0.008 Nm/rd, 0.000001 Nm/rd and 0.08 Nm/rd, respectively. Δt is the time step, adopted as 1 s and $\boldsymbol{\theta}$ is the attitude error with respect to the orbital frame (whose axes are the local vertical, close to the satellite velocity vector and orthogonal to the orbit plane), in small Euler angles.

3 MOMENTUM DUMPING

The employed reaction wheel desaturation strategy was the Conventional Cross Product Law (CCPL), which can be calculated by [7]:

$$\mathbf{M} = g\,\boldsymbol{\Delta h}\times\mathbf{B}\,, \tag{7}$$

where g is the control gain, $\boldsymbol{\Delta h}$ is the reaction wheel angular momentum and $\mathbf{B}$ is the Earth's magnetic field vector. This provides a continuous torque magnitude which can be achieved by means of a PWM (Pulse Width Modulation) switching of the magnetorquers. However, the PWM causes stress on the magnetorque hardware and compromises the magnetic cleanliness of the satellite. Therefore, to avoid the PWM strategy a discrete bang-bang (on-off) control was also tested.

The bang-bang control law can be adapted from Equation 7:

$$\mathbf{M}_B = C\frac{(\boldsymbol{\Delta h}\times\mathbf{B})}{|\boldsymbol{\Delta h}\times\mathbf{B}|}, \tag{8}$$

where C is the maximum dipole strength of the magnetorquers.

In order to improve the momentum dumping strategy, a dead zone was also implemented:

$$Z = \left|\boldsymbol{\Delta}\hat{\mathbf{h}}\times\hat{\mathbf{B}}\right| \tag{9}$$

It was considered that the magnetic torque of the satellite is much higher than the torques due to the periodic disturbances, so only the secular torques were taken into account.

4 ATTITUDE AND BIAS ESTIMATION

The conventional Kalman Filter for linear systems has two steps: the prediction and update. The prediction step is calculated using the following discrete equations [8]:

$$\bar{\mathbf{x}}_k = \boldsymbol{\Phi}_{k,k-1}\,\hat{\mathbf{x}}_{k-1}, \tag{10}$$

$$\bar{\mathbf{P}}_k = \boldsymbol{\Phi}_{k,k-1}\,\hat{\mathbf{P}}_{k-1}\,\boldsymbol{\Phi}_{k,k-1}^T + \boldsymbol{\Gamma}_k\,\mathbf{Q}_k\,\boldsymbol{\Gamma}_k^T\,, \tag{11}$$

where $\hat{\mathbf{x}}_{k-1}$ and $\hat{\mathbf{P}}_{k-1}$ are the last updated states and covariance, respectively, $\boldsymbol{\Phi}_{k,k-1}$ is the state transition matrix and $\boldsymbol{\Gamma}_k$ is the additive dynamic noise matrix.

For the update step, the equations are:

$$\mathbf{K}_k = \overline{\mathbf{P}}_k \, \mathbf{H}_k^T \left(\mathbf{H}_k \, \overline{\mathbf{P}}_k \, \mathbf{H}_k^T + \mathbf{R}_k \right)^{-1}, \tag{12}$$

$$\hat{\mathbf{P}}_k = \left(\mathbf{I} - \mathbf{K}_k \, \mathbf{H}_k \right) \overline{\mathbf{P}}_k , \tag{13}$$

$$\hat{\mathbf{x}}_k = \overline{\mathbf{x}}_k + \mathbf{K}_k \left(\mathbf{y}_k - \mathbf{H}_k \, \overline{\mathbf{x}}_k \right), \tag{14}$$

where $\mathbf{K}_k$ is the Kalman Gain, $\mathbf{H}_k$ is the measurement matrix, $\mathbf{I}$, an identity matrix $\mathbf{y}_k$ the measures and $\mathbf{R}_k$ the covariance matrix.

For the attitude represented by quaternions (**q**) and gyroscope bias (**b**) estimations, it is common to use the following state equations, composed by seven elements:

$$\dot{\mathbf{x}} = \begin{bmatrix} \dot{\mathbf{q}} \\ \dot{\mathbf{b}} \end{bmatrix} = \begin{bmatrix} \frac{1}{2} \boldsymbol{\Omega} \, \mathbf{q} \\ \mathbf{0} \end{bmatrix} + \mathbf{w} , \tag{15}$$

where **w** represents the model uncertainties, modelled by a white noise with covariance **Q** and **Ω** is defined as in Equation 4.

Considering the angular velocity vector constant between two consecutive measures, the quaternion transition matrix can then be calculated as [9]:

$$\boldsymbol{\Phi}_{q|k+1,k} = \cos\left(\frac{|\boldsymbol{\omega}| \Delta t}{2} \right) \mathbf{I}_{4\times4} + \frac{1}{|\boldsymbol{\omega}|} \operatorname{sen}\left(\frac{|\boldsymbol{\omega}| \Delta t}{2} \right) \boldsymbol{\Omega}(\boldsymbol{\omega}) \tag{16}$$

which is easier to implement because it avoids numerical integration of the state.

Since the quaternion has unity module, it causes a singularity in the covariance matrix, which is a known disadvantage of using quaternions for attitude estimation:. Due to this singularity, the Kalman filter has to be adapted. In this work, the solution adopted was the reduced order covariance matrix [9].

4.1 REDUCED ORDER COVARIANCE

In order to reduce the order of the quaternion covariance matrix (7x7), the following matrix transformation shall be applied:

$$\mathbf{P}^r = \mathbf{S}^T(\mathbf{q}) \mathbf{P} \, \mathbf{S}(\mathbf{q}) \text{ and } \mathbf{Q}^r = \mathbf{S}^T(\mathbf{q}) \mathbf{Q} \, \mathbf{S}(\mathbf{q}), \tag{17}$$

where $\mathbf{P}^r$ and $\mathbf{Q}^r$ are the reduced order covariance matrices (6x6) and **S** is calculated as:

$$\mathbf{S}(\mathbf{q}) = \begin{pmatrix} \boldsymbol{\Xi}(\mathbf{q}) & \mathbf{0}_{4\times3} \\ \mathbf{0}_{3\times3} & \mathbf{I}_{3\times3} \end{pmatrix}, \text{ with } \boldsymbol{\Xi}(\mathbf{q}) = \begin{pmatrix} \eta & -\varepsilon_3 & \varepsilon_2 \\ \varepsilon_3 & \eta & -\varepsilon_1 \\ -\varepsilon_2 & \varepsilon_1 & \eta \\ \varepsilon_1 & -\varepsilon_2 & -\varepsilon_3 \end{pmatrix}, \tag{18}$$

which is a function of the quaternion elements $\mathbf{q} = (\varepsilon_1 \;\; \varepsilon_2 \;\; \varepsilon_3 \;\; \eta)^T$.

The reduced covariance matrix is then propagated using the discrete Riccati equation, where the transition matrix also must have its order reduced [10]:

$$\overline{\mathbf{P}}_{k+1}^{r} = \widetilde{\mathbf{\Phi}}\,\overline{\mathbf{P}}_{k}^{r}\,\widetilde{\mathbf{\Phi}}^{T} + \int_{t_k}^{t_{k+1}} \widetilde{\mathbf{\Phi}}\,\mathbf{Q}^{r}\,\widetilde{\mathbf{\Phi}}^{T} dt\,. \tag{19}$$

with,

$$\widetilde{\mathbf{\Phi}} = \begin{pmatrix} \mathbf{\Lambda} & \mathbf{K}^{*} \\ \mathbf{0}_{3\times3} & \mathbf{I}_{3\times3} \end{pmatrix}_{6x6}, \tag{20}$$

$$\mathbf{\Lambda} = \mathbf{\Xi}^{T}(\overline{\mathbf{q}}_{k+1})\mathbf{\Phi}_{q}(\hat{\boldsymbol{\omega}}_{k})\mathbf{\Xi}(\hat{\mathbf{q}}_{k}) \text{ and } \mathbf{K}^{*} = -\frac{1}{2}\int_{t_k}^{t_{k+1}} \mathbf{\Lambda}\, dt \tag{21}$$

For the covariance matrix update phase, the equations were modified as follows [10]:

$$\widetilde{\mathbf{H}}_{k} = \mathbf{H}_{k}\,\mathbf{S}(\overline{\mathbf{q}}_{k}), \tag{22}$$

$$\widetilde{\mathbf{K}}_{k} = \overline{\mathbf{P}}_{k}^{r}\,\widetilde{\mathbf{H}}_{k}^{T}\left(\widetilde{\mathbf{H}}_{k}\,\overline{\mathbf{P}}_{k}^{r}\,\widetilde{\mathbf{H}}_{k}^{T} + \mathbf{R}_{k}\right)^{-1}, \tag{23}$$

$$\hat{\mathbf{P}}_{k}^{r} = \left(\mathbf{I}_{6\times6} - \widetilde{\mathbf{K}}_{k}\,\widetilde{\mathbf{H}}_{k}\right)\overline{\mathbf{P}}_{k}^{r}\,. \tag{24}$$

To update the states, the Kalman gain also must return to full order:

$$\mathbf{K}_{k} = \mathbf{S}(\overline{\mathbf{q}}_{k})\widetilde{\mathbf{K}}_{k}\,. \tag{25}$$

Then, the states are updated using Equation 14.

After the calculation of the states, the angular velocity can then be reconstructed, allowing a better control of the spacecraft during the passages in the Earth's shadow:

$$\boldsymbol{\omega} = \tilde{\boldsymbol{\omega}} - \hat{\mathbf{b}} \tag{26}$$

where $\tilde{\boldsymbol{\omega}}$ is the gyroscope measurement.

5 SIMULATION RESULTS

Initial conditions for the simulations were: circular orbit, inclination of 25° and an altitude of 630Km. Attitude in Euler angles at beginning simulation was adopted as 60°, 30° and 40° and body angular velocities were set at 0.6 rpm, 0.3 rpm e 0.9 rpm. Reaction wheels speed started at 0 rpm.

Simulation time was set to 18000 s, which is approximately three orbits, to allow the Kalman filter to converge to a stable estimate for the bias. The satellite passages through the Earth's shadow occurred at 2237 sec to 4374 sec in the first orbit, 8065 sec to 10200 sec in the second and 13890 sec to 16030 sec in the third orbit.

The gyroscope bias and noise level were set at constant 50°/h and 5°/h for all axes, respectively, and the disturbance torque considered was a residual magnetic moment, with

magnitude 0.01 Am^2, which is a high value considering the spacecraft characteristics, but it allows to validate the control strategies and momentum dumping.

The results for the attitude error and estimated bias are shown in Figures 2 and 3. Figure 2 shows the Euler angle of a Euler axis and angle attitude. Since the Euler angle is null for a null attitude, this angle can be understood also as an error angle. The PID controller managed to keep the pointing accuracy lower than 5° and the bias estimated by the Kalman filter remained inside 5° deviation. The attitude presented a larger error during the first passage through the Earth's shadow, on account of the still converging bias.

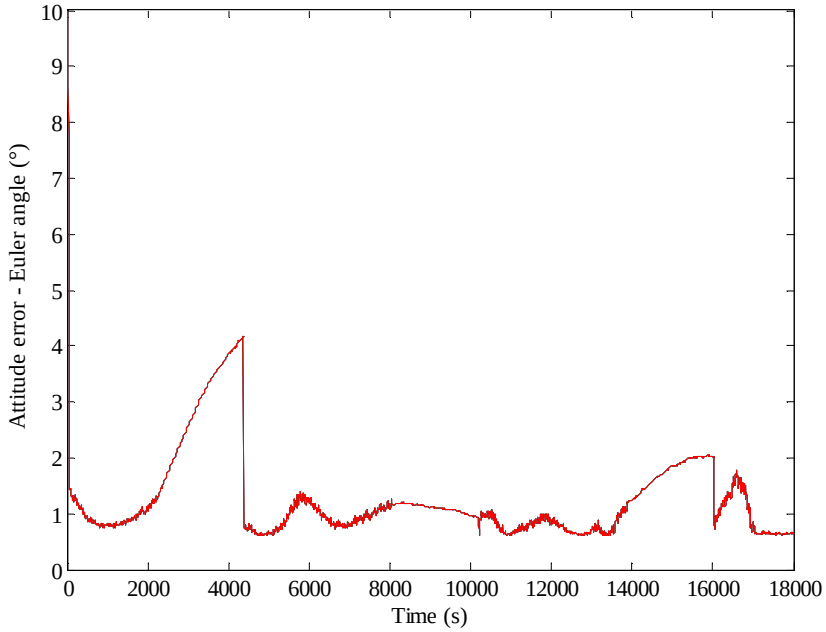

Figure 2: Attitude error in Euler angle

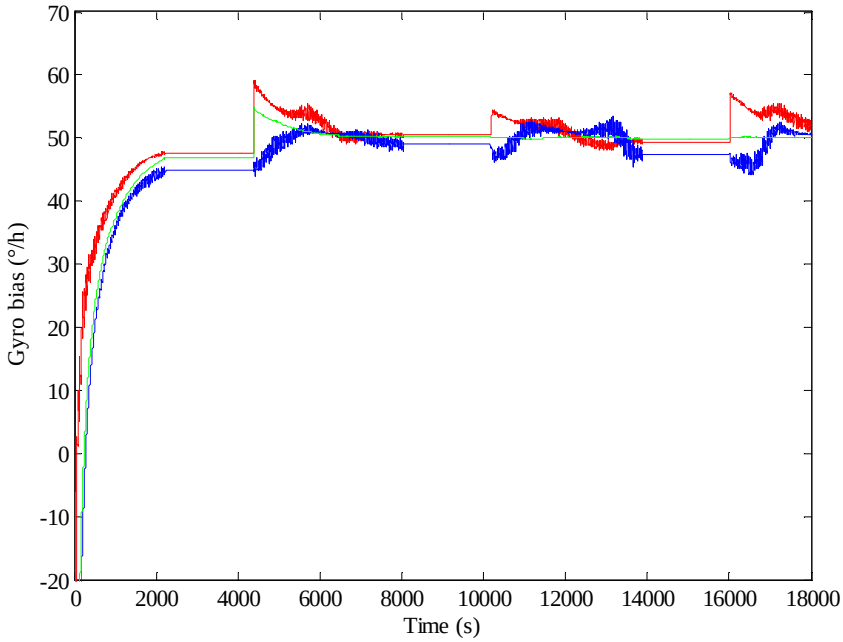

Figure 3: Estimated gyroscope bias by the Kalman filter

The reaction wheel speeds for each of the simulations are shown in Figure 4. It can be noted that, without the desaturation, the wheel speeds are increasing toward saturation (a), but with the CCPL (b) and bang-bang (c) desaturation techniques, the wheel angular rates were brought close to the reference speed (null speed). Subtracting the results of CCPL and bang-bang techniques (d), the maximum difference in the wheel's speed is about 100 rpm, corresponding to 1% of the maximum supported wheel speed. Comparing the total energy spent, calculated by the integral of the quadratic magnetic moment (e), it can be noted that CCPL (blue line) is about 20% lower than bang-bang (red line). This leads to a better performance per energy in the CCPL strategy.

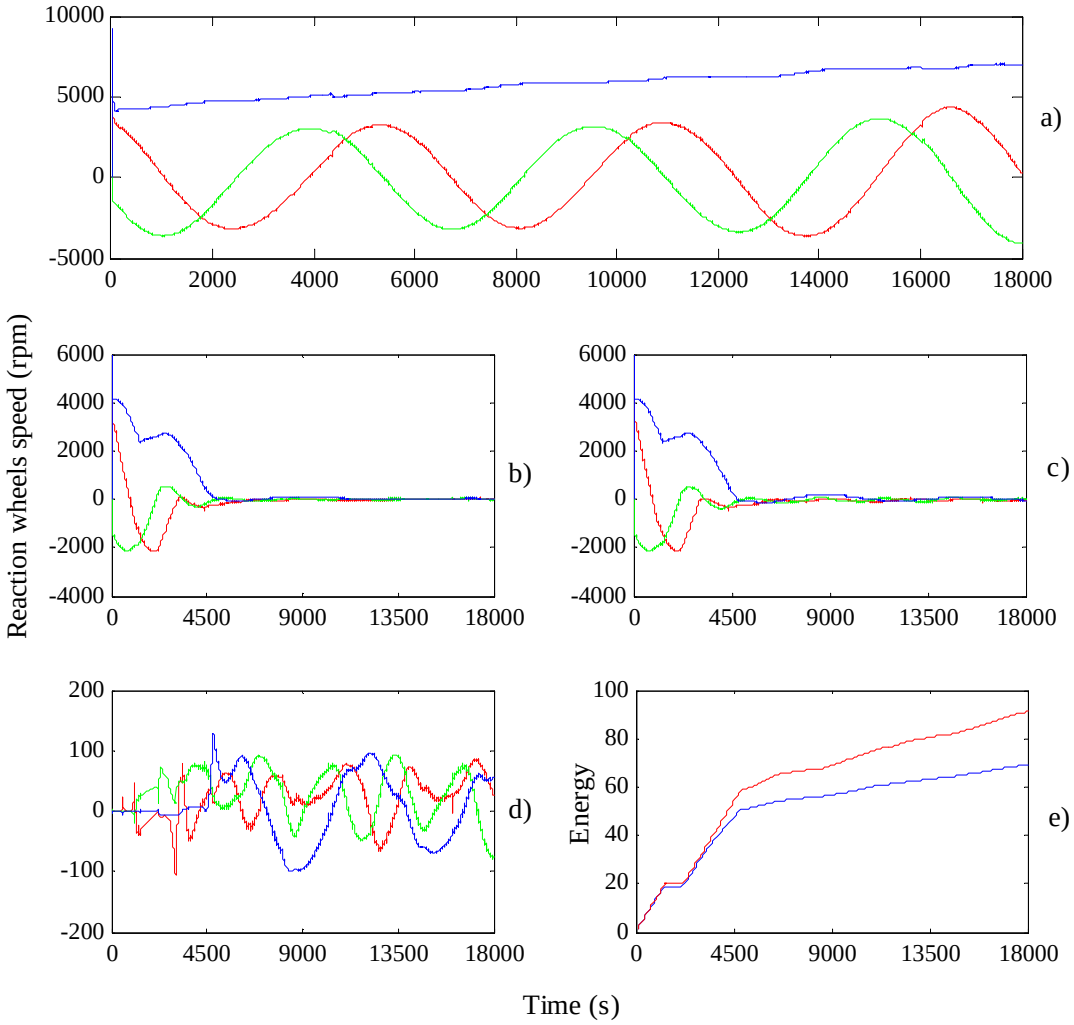

Figure 4: Reaction wheel speeds: a) without desaturation, b) with CCPL, c) with bang-bang technics, d) the difference between CCPL and bang-bang and e) the total energy spent with CCPL (blue line) and bang-bang (red line).

6 CONCLUSIONS

This work presented the CONASAT nanosatellite configuration, as well its attitude control components and equations of motion. The attitude quaternion is computed by a TRIAD algorithm based on measures of a magnetometer and coarse sun sensors. A Kalman filter provides the attitude quaternion and gyroscope bias estimation for a PID controller acting on a

set of 3 reaction wheels. For the wheel desaturation strategy, the basic equations for the CCPL and bang-bang methods were analyzed and compared, and could be noted that CCPL presented a very close performance to bang-bang with less energy consumption. The implemented Kalman filter, which was used to estimate attitude represented by quaternion and gyroscope bias, was adapted to avoid the covariance matrix singularity, an inherent problem when using quaternions.

The results have shown that the methods applied here achieved the goals of attitude error (5°) and the desaturation of the reaction wheel angular momentum.

7 REFERENCES

[1] WERTZ, J. R. Space Mission Analysis and Design. Microcosm Press, 1999.

[2] INSTITUTO NACIONAL DE PESQUISAS ESPACIAIS. Constelação de Nano Satélites para Coleta de Dados Ambientais – Documento de Descrição da Missão (DDM). CNS-DDM-001. 2011.

[3] CARRARA, V.; KUGA, H. K.; BRINGHENTI, P. M.; CARVALHO, M. J. M. Attitude Determination, Control and Operating Modes for CONASAT Cubesats. 24th International Symposium on Space Flight Dynamics (ISSFD), Laurel, Maryland, 2014.

[4] HUGHES, P. C. Spacecraft Attitude Dynamics. Dover Books, 1986.

[5] WERTZ, J. R. Spacecraft Attitude Determination and Control. D. Reidel Publishing, 1978.

[6] CARRARA, V. Cinemática e Dinâmica de Satélites Artificiais", São José dos Campos: Instituto Nacional de Pesquisas Espaciais, 2012.

[7] CAMILLO, P.; MARKLEY, F. L. Orbit-Averaged Behavior of Magnetic Control Laws for Momentum Unloading. Journal of Guidance and Control, Vol. 3, No. 6, pp. 563-568, 1980.

[8] KUGA, H. K. Noções Práticas de Técnicas de Estimação. Instituto Nacional de Pesquisas Espaciais, São José dos Campos/SP, 2005.

[9] LEFFERTS, E. J.; MARKLEY, F. L.; SHUSTER, M. D. Kalman Filtering for Spacecraft Attitude Estimation. Journal of Guidance, Control and Dynamics, Vol. 5, No. 5, p. 417, 1982.

[10] GARCIA, R. V.; KUGA, H. K.; ZANARDI, M. C. Filtro Não Linear de Kalman Sigma-Ponto com Algoritmo Unscented Aplicado a Estimativa Dinâmica da Atitude de Satélites Artificiais. São José dos Campos, SP, 2011.